Reducing Power Consumption of Active-Matrix Mini-LED Backlit LCDs by Driving Circuit

Ming-Yang Deng, En-Lin Hsiang, Qian Yang, *Graduate Student Member, IEEE*, Chia-Ling Tsai, Bo-Shu Chen, Chia-En Wu, Ming-Hsien Lee, Shin-Tson Wu, *Fellow, IEEE*, and Chih-Lung Lin, *Member, IEEE*

***Abstract*— An active-matrix (AM) driving circuit using a low-temperature poly-silicon thin-film transistor (LTPS TFT) is developed to reduce the power consumption of mini-light-emitting diode (LED) backlit liquid-crystal displays (LCDs). By lowering the drain–source voltage (V_{DS}) of the switching TFT on the driving current path, the range of required voltage across the proposed circuit can be reduced, decreasing the power consumption of the mini-LED backlight. The proposed circuit also can compensate for V_{TH} variation in the LTPS TFT and the *I–R* rise of V_{SS} to provide a uniform driving current to flow through the mini-LED. By measuring the *I–V* curves of a fabricated LTPS TFT, we build a reliable simulation model and compare the proposed circuit to that of the state-of-the-art. Simulated results indicate that the proposed circuit can improve the power consumption by 16.67% and reduce the current error rates below 8% when the V_{TH} of TFT varies by ±0.3 V and V_{SS} rises +1 V. Measured results further confirm that the V_{DS} of the switching TFT is reduced by 2.208 V compared to a 6T2C compensating circuit. Therefore, widespread applications of the proposed circuit for AM mini-LED backlit LCDs to produce high-dynamic-range images are foreseeable.**

***Index Terms*— Active-matrix (AM), current–resistance rise/drop, low-temperature poly-silicon (LTPS), mini-light-emitting diode (LED) backlit liquid-crystal display (LCD), power consumption, thin-film transistors (TFTs), threshold voltage (V_{TH}).**

Manuscript received February 10, 2021; accepted March 17, 2021. Date of publication April 1, 2021; date of current version April 22, 2021. This work was supported in part by the Advanced Optoelectronic Technology Center, National Cheng Kung University, Tainan, Taiwan, in part by the Ministry of Science and Technology (MOST) of Taiwan under Project 109-2622-E-006-019-CC2, and in part by the AU Optronic Corporation. The review of this article was arranged by Editor X. Guo. *(Corresponding author: Chih-Lung Lin.)*

Ming-Yang Deng and Chia-Ling Tsai are with the Department of Electrical Engineering, National Cheng Kung University, Tainan 70101, Taiwan.

En-Lin Hsiang, Qian Yang, and Shin-Tson Wu are with the College of Optics and Photonics, University of Central Florida, Orlando, FL 32816 USA.

Bo-Shu Chen is with Novatek Microelectronics Corporation, Hsinchu 30070, Taiwan.

Chia-En Wu and Ming-Hsien Lee are with AU Optronics Corporation, Hsinchu 30078, Taiwan.

Chih-Lung Lin is with the Department of Electrical Engineering, National Cheng Kung University, Tainan 70101, Taiwan, and also with the Advanced Optoelectronic Technology Center, National Cheng Kung University, Tainan 701-01, Taiwan (e-mail: cllin@ee.ncku.edu.tw).

Color versions of one or more figures in this article are available at https://doi.org/10.1109/TED.2021.3067860.

Digital Object Identifier 10.1109/TED.2021.3067860

I. Introduction

DISPLAY is an important human–machine interface. Its widespread applications range from smartwatches, smartphones, pads, computers, TVs, public display boards, to vehicles, just to name a few. Presently, liquid-crystal displays (LCDs) and organic light-emitting diode (OLED) displays are dominating, while micro-light-emitting diodes (LEDs) are emerging [1], [2]. OLED is an emissive display so that its contrast ratio is much higher than that of LCD. Moreover, its thin profile enables flexible and rollable displays. However, its lower brightness and much shorter lifetime limit its applications.

LEDs with high efficiency, high brightness, and long lifetime have been widely used in public lightings, outdoor display boards, traffic lights, automotive lighting, and an LCD backlight unit (BLU). Recently, shrinking the LED size to millimeters (called mini-LED) and microns (called μLED) has attracted much attention for flat panel displays [3]–[6]. An important application of mini-LED is as LCD's BLU to achieve high dynamic range (HDR). By using a direct-lit mini-LED array with sufficient local dimming zones [7], such an LCD can achieve a comparable contrast ratio with an OLED, while keeping high brightness and long lifetime. Hence, many mini-LED backlit HDR LCD products are emerging, such as notebooks, pads, gaming monitors, and TVs. However, several of these mini-LEDs are driven by passive matrix (PM) [8], [9]. To achieve HDR images, 100–1000 s of mini-LED dimming zones are required to suppress the halo effects, depending on the LCD's native contrast ratio. A PM BLU increases the size and complexity of a printed circuit board (PCB) and the number of source ICs, increasing the cost of the panel [10].

On the other hand, an active-matrix (AM) that is based on a thin-film transistor (TFT) backplane [11]–[14] can eliminate the need for considerable ICs to drive the mini-LEDs, keeping down the cost of the panel. Nevertheless, to realize an AM mini-LED BLU for LCD applications, issues of power consumption and uniformity of luminance need to be considered. To achieve the required luminance, say 500 nits, of the image, the driving current of the mini-LED must be increased to several milli-Ampere (mA) because of the low transmittance (5%–7%) of the LCD. With such a high driving current, the power consumption and current–resistance (*I–R*) drop/rise in the power source lines become severe issues.

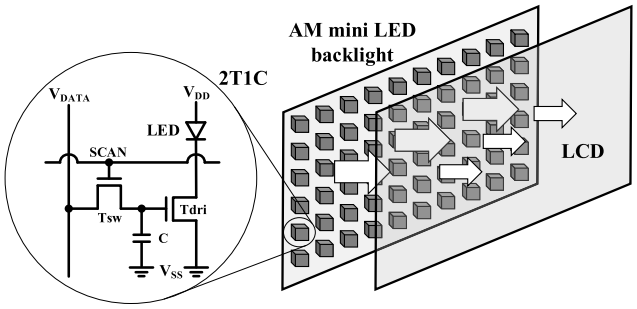

Fig. 1. 2T1C driving circuit used in AM mini-LED BLU [11], [12], [14].

Liu *et al.* [11] reported a mini-LED backlight with four LEDs in series in a dimming zone to reduce the required driving current of the backlight, ameliorating the variations of V_{DD} and V_{SS} that are caused by the I–R drop/rise. This method, however, substantially increases the cost of the product due to the use of more mini-LEDs. Without increasing the number of mini-LEDs, adding an additional metal layer and optimizing the current-crowding path [12] also can reduce the voltage variation in the power source lines. To reduce the power loss associated with the TFTs, the aspect ratio of the driving TFT can be increased to reduce its equivalent resistance [13]. However, doing so makes the differentiation of gray levels at low luminance difficult. With respect to the driving circuit, mini-LEDs are currently driven by conventional 2T1C [11], [12], [14], which cannot produce a uniform driving current for a mini-LED BLU owing to the variations in the electrical characteristic of the TFT and I–R drop/rise in the power source lines, as shown in Fig. 1. Although compensating pixel circuits [15], [16] in an AM mini-LED display can ameliorate the aforementioned problems, they cannot substantially reduce the power consumption of the BLU.

This work presents an AM driving circuit for reducing the power consumption of mini-LED backlit LCDs by reducing the total voltage across the proposed circuit. The proposed circuit also compensates for variations in the threshold voltage (V_{TH}) of a low-temperature poly-silicon TFT (LTPS TFT) and the V_{SS} power line, ensuring the high uniformity of the driving currents of all mini-LEDs over the backlight. The compensation for the V_{TH} variation and the I–R rise of V_{SS} and the reduction of the power consumption are verified experimentally.

II. Mechanism of Compensating Circuit and Characteristics of Switching TFT

Since the LTPS TFT has high field-effect mobility, small layout area, and high reliability, it is suitable for use in the backplane of an AM array of a high-end display. However, variations in the electrical characteristics of an LTPS technology, such as V_{TH}, make the driving current of the emissive device nonuniform, degrading the quality of the display image [17], [18].

A diode-connection scheme has been commonly implemented in the pixel circuit of an AMOLED display to compensate for the V_{TH} variation of LTPS TFT [19]–[25], as shown in Fig. 2. By connecting two TFTs, Tsw1 and Tdri, to act like a diode, the charge stored in the capacitor discharges

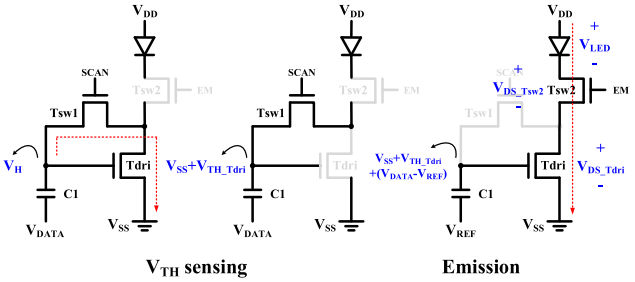

Fig. 2. Diode-connected scheme used in AMOLED pixel circuit.

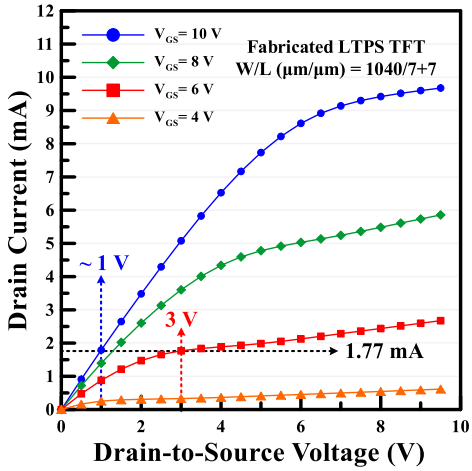

Fig. 3. Measured I_D–V_{DS} transfer curves of LTPS TFT with W/L = 1040 μm/(7 + 7) μm at V_{GS} = 4, 6, 8, and 10 V.

through the TFTs until the potential difference between the gate and source nodes of the Tdri is close to its V_{TH}. Tdri is the driving TFT that operates in the saturation region to generate a stable current to drive a mini-LED. Hence, the V_{TH} variation in LTPS TFTs can be sensed and stored in a capacitor. Notably, in this scheme, a switching TFT, Tsw2, is needed to block any current that would flow through the emissive device before the emission period begins, avoiding undesired emission. The voltage across the circuit is the sum of the drain–source voltage (V_{DS}) of the TFTs and the forward voltage of the mini-LED. Since the driving current of the mini-LED as BLU is much larger than that in the AMOLED pixel circuit, increasing the number of TFTs on the current path drastically increases the static power, according to $P_{static} = I_D \times V_{total} \times$ emission duty, where V_{total} is the sum of V_{DS} values of the switching and the driving TFTs and the forward voltage of the mini-LED. The V_{DS} of the switching TFT, however, can be reduced by increasing its gate–source voltage (V_{GS}). Fig. 3 plots the measured I_D–V_{DS} curves of a fabricated TFT. At a fixed current of 1.77 mA, V_{DS} falls by 2 V as V_{GS} increases from 6 to 10 V. Since the total voltage across the circuit is reduced, the power consumption is improved. Accordingly, this work proposes a mini-LED driving circuit to increase the V_{GS} of the switching TFT to reduce the power consumption of the AM mini-LED backlight.

III. Proposed Mini-LED Driving Circuit

Fig. 4(a) schematically depicts the proposed mini-LED driving circuit, which consists of eight TFTs and

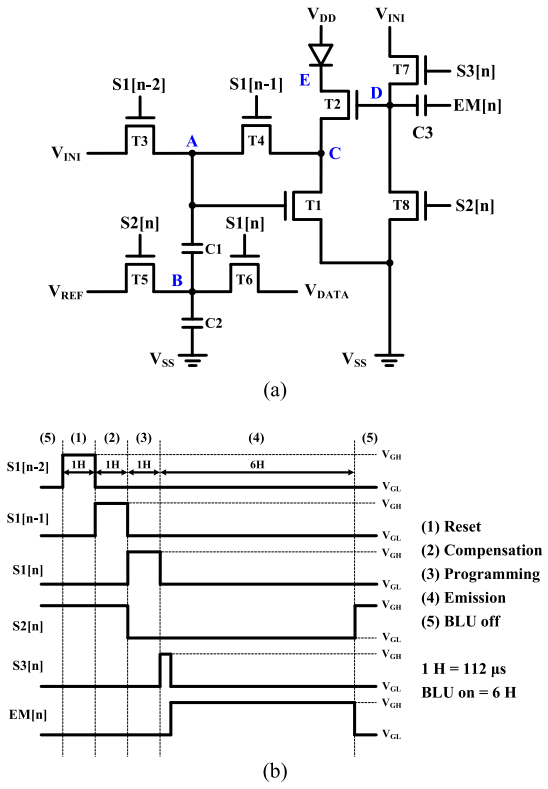

Fig. 4. (a) Schematic and (b) timing diagram of proposed mini-LED driving circuit.

three capacitors. T1 is the driving TFT, which controls the current that flows through the mini-LED, and T2 to T8 are the switching TFTs. $C1$–$C3$ are the storage capacitors. Herein, T7 and $C3$ are used to increase the gate voltage of T2 to reduce its V_{DS}. Fig. 4(b) shows the timing diagram of each controlling signal [S1[$n-2$] – [n], S2[n], S3[n], and electromagnetic (EM)]. The operation of the proposed circuit can be divided into reset, compensation, programming, emission, and BLU off phases.

A. Reset Phase

S1[$n-2$] and S2[n] are high to turn on T1, T3, T5, and T8. Node A is reset to V_{INI} to activate T1, discharging node C to V_{SS}, and node B is charged to V_{REF} through T5. Herein, since node D is discharged to V_{SS} through T8, T2 can be turned off to prevent the flow of any current through the mini-LED.

B. Compensation Phase

S1[$n-2$] goes low to turn off T3, and S1[$n-1$] goes high to turn on T4. Node A is discharged to $V_{SS}+V_{TH\_T1}$ through T1 and T4 when T1 is turned off. Herein, V_{TH_T1} is the threshold voltage of T1. Therefore, the V_{SS} and V_{TH} variation in the driving TFT of each mini-LED driving circuit can be sensed and stored in $C1$.

C. Programming Phase

S1[$n-1$] and S2[n] become low to turn off T4, T5, and T8. Since S1[n] becomes high to turn on T6, node B can be charged from V_{REF} to V_{DATA}. Based on the charge conservation of a capacitor, the voltage of node A is boosted by $C1$ as follows:

$$V_A = V_{SS} + V_{TH\_T1} + (V_{DATA} - V_{REF}). \tag{1}$$

Thus, the data voltage is stored at node A. The V_{GS} of T1 can be expressed as the following equation:

$$\begin{aligned} V_{GS} &= V_{SS} + V_{TH\_T1} + (V_{DATA} - V_{REF}) - V_{SS} \\ &= V_{TH\_T1} + (V_{DATA} - V_{REF}). \end{aligned} \tag{2}$$

D. Emission Phase

At the beginning of this phase, V_{INI} is applied to node D through T7 when S3 goes high, so T2 is turned on. After that, node D is coupled to $V_{INI}+(V_{GH}-V_{GL})$ by $C3$ when EM changes from V_{GL} to V_{GH}. As described in Section II, since the V_{GS} of T2 is increased, the required V_{DS} of T2 is reduced. The driving current that is generated by T1 can be expressed as follows:

$$\begin{aligned} I_{LED} &= \frac{1}{2}\mu C_{OX}\frac{W}{L}(V_{GS} - V_{TH})^2 \\ &= \frac{1}{2}\mu C_{OX}\frac{W}{L}[(V_{DATA} - V_{REF}) + V_{TH\_T1} - V_{TH\_T1}]^2 \\ &= \frac{1}{2}\mu C_{OX}\frac{W}{L}(V_{DATA} - V_{REF})^2 \end{aligned} \tag{3}$$

where μ, C_{OX}, W, and L are the field-effect mobility, gate oxide capacitance per unit area, channel width, and channel length of T1. As shown in (3), since V_{TH_T1} and V_{SS} are stored in $C1$, the driving current is immune to the V_{TH} variation and V_{SS} rise. The uniformity of the current that flows through each mini-LED is, thus, ensured.

E. BLU off Phase

S2[n] goes high again to turn on T5 and T8. Node D is reset to V_{SS} to turn off T2 to avoid the flow of any current through the mini-LED. Notably, the voltage of node A is reduced to $V_{SS}+V_{TH\_T1}$ to turn off T1 since node B is discharged to V_{REF} through T5. Hence, the BLU is turned off.

According to the aforementioned operation, the proposed mini-LED driving circuit consumes less power than the AMOLED pixel circuit because it has a lower V_{DS} of the switching TFT that is placed on the driving current path. The proposed circuit can also compensate for the V_{TH} and the V_{SS} I–R rise variations and ensure that no current flows through mini-LED before the emission phase, increasing the uniformity of the light from the mini-LED backlight.

IV. Results and Discussion

The feasibility of the proposed mini-LED driving circuit is verified using an HSPICE simulator with the Rensselaer Polytechnic Institute (RPI) poly-Si TFT model (level = 62). To build a simulation model, the characteristics of the fabricated LTPS TFTs are measured and fitted, as shown in Fig. 5. Table I presents the simulated parameters, including the aspect ratio of the TFTs, the capacitances of the capacitors, the voltage levels of the power sources, and the voltage swing

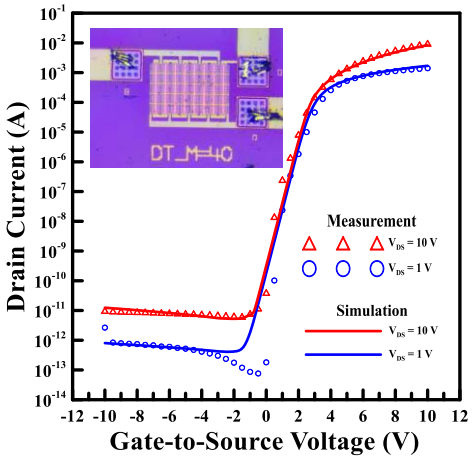

Fig. 5. Measured and simulated I_D–V_{GS} transfer curves of LTPS TFT with $W/L = 1040\ \mu m/(7 + 7)\ \mu m$.

TABLE I
PARAMETERS OF PROPOSED DRIVING CIRCUIT

TFT & Capacitance			
Parameter	Value	Parameter	Value
T1 (μm/μm)	1040/(7+7)	C1 (pF)	5
T2 (μm/μm)	1040/(7+7)	C2 (pF)	5
T3-T8 (μm/μm)	6/(3+3)	C3 (pF)	1
Scan, EM & Power source			
Parameter	Value	Parameter	Value
V_{DD} (V)	9	V_{SS} (V)	-3
V_{INI} (V)	3	V_{REF} (V)	0
V_{DATA} (V)	0 ~ 5.14	S1-S3,EM (V)	-7 ~ 9

of each scan signal. Since the mini-LEDs are driven by a high current of 2 mA, the driving TFT is composed of two TFTs with an aspect ratio of 1040 μm/(7 + 7) μm that are connected in series to reduce the stress of the driving TFT. The designed parameters are based on an AM 48 × 48 mini-LED backlit module (2304 dimming zones) with an operating frequency of 120 Hz for use in a 2.89-in virtual reality (VR) LCD with a resolution of 3456 × RGB × 3456 and a frame rate of 90 Hz. To eliminate the motion blur of the VR display, each mini-LED emits for only 672 μs to reduce the moving-picture response time [26].

A. Compensation for V_{TH} Variation and V_{SS} I–R Rise

To validate the effectiveness of the proposed circuit in compensating for the V_{TH} variation, Fig. 6(a) plots the simulated transient voltage waveforms at node A when the V_{TH} of the driving TFT is shifted by +0.3, 0, and −0.3 V. During the compensation phase, the voltages at node A are discharged to −1.880, −2.177, and −2.472 V, respectively, demonstrating that the circuit can successfully sense the variations of the V_{TH}. Fig. 6(b) plots the driving currents of the mini-LED and relative current error rates with different data voltage. The driving current that is generated by the proposed circuit increases with the data voltage from 2.38 to 5.14 V. The generated currents are almost equal, and the current error rates are all below 1.12%. Since a voltage change of the power source affects the stability of the driving current, 2 V

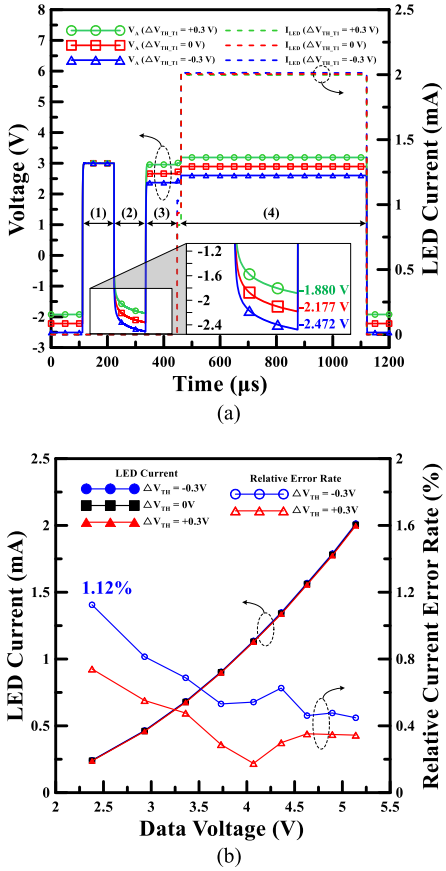

Fig. 6. (a) Simulated transient waveforms of V_A and (b) relative current error rates of proposed mini-LED driving circuit with different V_{TH} variations.

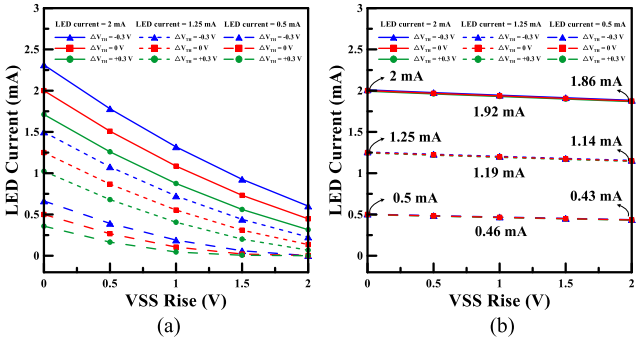

Fig. 7. Simulated relative current error rates of (a) conventional 2T1C and (b) proposed circuits with V_{TH} variations of ±0.3 V and 0 to V_{SS} rise of 2 V.

V_{SS} I–R rise and ±0.3 V V_{TH} variations are considered simultaneously to evaluate the feasibility of the proposed circuit. The conventional 2T1C circuit [11], [12], [14] and the proposed circuit are compared with respect to the V_{TH} variation and the V_{SS} I–R rise compensation in an AM mini-LED BLU. As shown in Fig. 7(a), the driving currents that are generated by the conventional 2T1C circuit change drastically when V_{SS} rises 2 V. In contrast, the relative current error rates of the proposed circuit are less than 7%, 8.8%, and 14% at high, medium, and low gray levels, respectively. Notably, the V_{SS} rise of 2V is considered to be the worst case for analyzing the reliability of the proposed circuit. The rise of the voltage

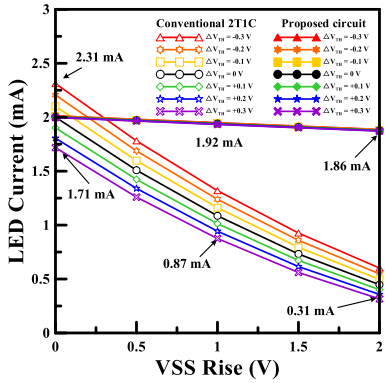

Fig. 8. Simulated driving currents of 2 mA when V_{TH} varies from −0.3 to +0.3 V and V_{SS} varies from 0 to +2 V.

of the V_{SS} power source can be further reduced to below 2 V by adding an additional metal layer or optimizing the current-crowding path [12]. Since the V_{TH} of each LTPS TFT may vary over the whole substrate, Fig. 8 plots the simulated driving currents, considering variations of V_{TH} of −0.3, −0.2, −0.1, 0, +0.1, +0.2, and +0.3 V and variation of V_{SS} of 2 V when the initial driving current is 2 mA. The relative current error rates of the 2T1C circuit are up to 84.5%, while those of the proposed circuit are less than 7%. Notably, the driving currents of the proposed circuit remain highly uniform and overlapping even if the V_{TH} of the driving TFT varies from −0.3 to 0.3 V.

To analyze the impact of variations in the driving currents on the luminance of the backlight, a LightTools simulator is utilized to simulate a mini-LED backlight with 288 dimming zones (48 × 6) in this work, as Fig. 9(a) depicts. The currents extracted from the simulated results are converted to the corresponding luminance of the mini-LED according to the luminance–current curve. The obtained luminance of each mini-LED is randomly placed on one of the 288 zones to simulate a mini-LED backlight. Fig. 9(b) and (c) shows the simulated brightness distribution of the mini-LED backlight when the 2T1C and the proposed circuits are used. In our optical simulation model using LightTools, a 48 × 6 mini-LED array with 1-mm pitch is employed, and a commercial diffuser film (Brightview C-HH80) is placed at 0.5 mm above the LED chip to eliminate hot spots. Then, we use a brightness enhancement film (3M Vikuiti BEFIII 90/50) to increase the luminance under a normal viewing angle. Finally, we use a spatial luminance meter to measure the uniformity. The size of spatial luminance meter (4 mm × 4 mm) is set to be smaller than the LED array (6 mm × 6 mm) to avoid nonuniformity in the edge region. Comparing Fig. 9(c) with Fig. 9(b), our proposed circuit dramatically improves the backlight uniformity (L_{max}/L_{min}) from 59% to 82%. As a result, by compensating for the V_{TH} variation and the V_{SS} rise, the proposed circuit can reduce the variation of the driving current and support the AM mini-LED BLU producing more uniform brightness for the LCD.

B. Power Consumption

According to the results that were presented in Section II, the V_{DS} of the TFT can be reduced by increasing its V_{GS}.

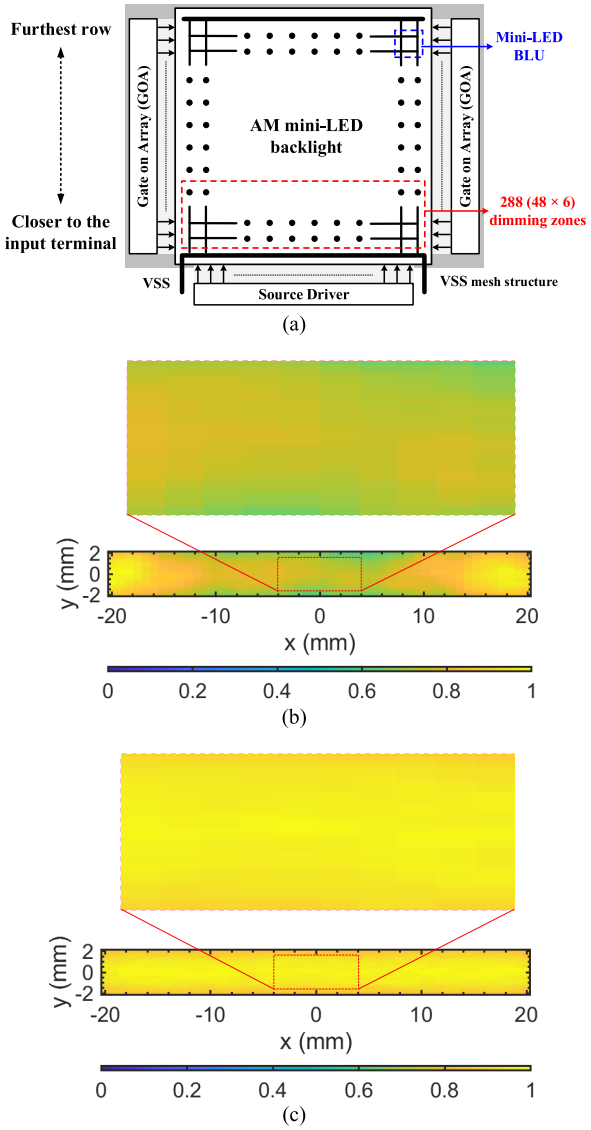

Fig. 9. (a) Diagram of mini-LED backlight with 288 dimming zones. Simulated brightness distribution of mini-LED backlight when (b) 2T1C and (c) proposed circuits are adopted.

However, the voltage range of the scan signals that are generated by the IC is limited, and a higher voltage level to drive the switching TFTs is not supported. Furthermore, the enlargement in the output range of the IC will increase the power that is consumed by the backlight. Thus, a capacitive coupling method is used in the proposed mini-LED driving circuit to increase the gate voltage of the switching TFT under the current specifications of the display system. To evaluate the reduction of the power consumption by the proposed circuit, the gate nodes of the switching TFT with and without that increase are compared. Fig. 10 shows the schematic and related timing diagrams of the proposed circuit in which T2 is directly connected to the EM signal. The simulated parameters are as in Table I. Fig. 11 plots the simulated transient waveforms of the mini-LED current (I_{LED}) at nodes A, C, D, E, and V_{SS} before and after the gate node of T2 is increased. Herein, the driving TFTs in both circuits have the same V_{GS} of ∼5.88 V and V_{DS} of ∼8.17 V to enable the

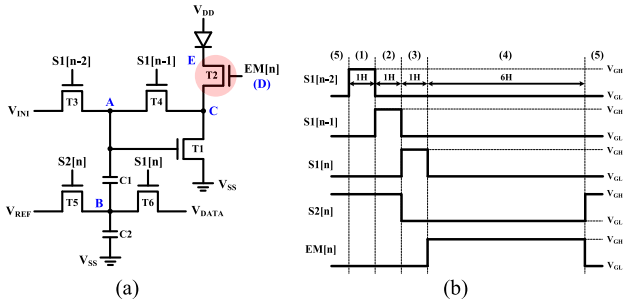

Fig. 10. (a) Schematic and (b) timing diagram of common diode-connected driving circuit.

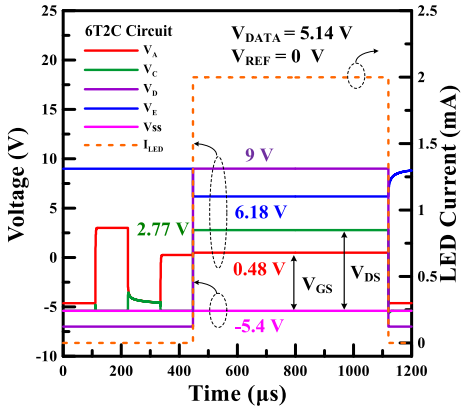

Fig. 11. Transient waveforms of I_{LED}, V_A, V_C, V_D, V_E, and V_{SS} of mini-LED driving circuit (a) before and (b) after the voltage of gate node of T2 is increased.

required voltage across the switching TFTs to be evaluated. Fig. 11(a) shows that when the driving current is 2 mA and the voltage at node D is 9 V, the voltages at nodes C and E are 2.77 and 6.18 V, respectively. Therefore, the voltage across the T2 is 3.41 V. By contrast, since the voltage at node D is raised to 16.57 V during the emission period, the V_{DS} of the T2 is only 1 V, as shown in Fig. 11(b). The total voltage across the TFTs on the driving current path is reduced by 2.4 V ($V_{EC\_6T2C} - V_{EC\_proposed} = 11.58\ V - 9.18\ V$). Table II lists the voltages of all nodes of T1 and T2 in both circuits. With the same V_{GS} and V_{DS} of T1, the total voltage across the 6T2C circuit must be increased to 14.4 V [9 V − (−5.4 V)] to achieve the same current of 2 mA. The power consumed by the proposed mini-LED driving

TABLE II
TRANSIENT VOLTAGES OF EACH NODE OF T1 AND T2

mini-LED current (I_{LED}) = 2 mA			
		6T2C circuit	Proposed circuit
T1	V_D (V)	2.77	5.18
	V_G (V)	0.48	2.89
	V_S (V)	-5.4	-3
T2	V_D (V)	6.18	6.18
	V_G (V)	9	16.57
	V_S (V)	2.77	5.18
V_{DD} (V)		9	9
V_{SS} (V)		-5.4	-3
Total voltage (V)		14.4	12

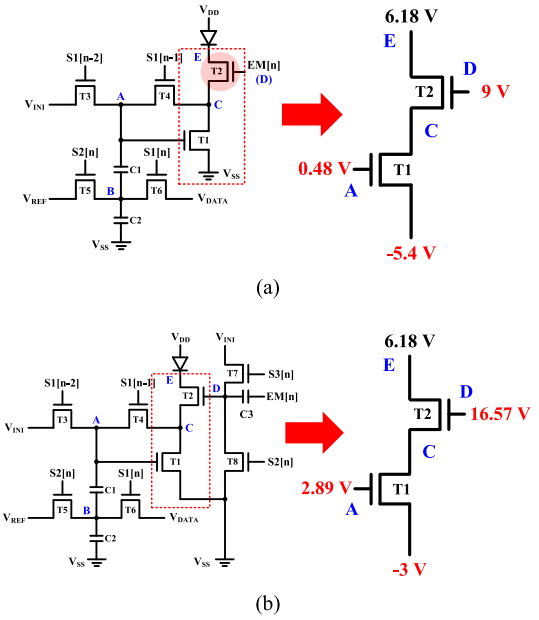

Fig. 12. Equivalent circuits of (a) 6T2C and (b) proposed circuits.

circuit is, thus, improved by 16.67%, as shown in the following equation:

$$\begin{aligned} P_{STATIC\_6T2C} &= 2\ mA \times 14.4\ V \times \text{Emission duty} \\ P_{STATIC\_PROPOSED} &= 2\ mA \times 12\ V \times \text{Emission duty} \\ \text{Improvement}(\%) &= \frac{P_{STATIC_{6T2C}} - P_{STATIC\_PROPOSED}}{P_{STATIC\_6T2C}} \times 100\%. \end{aligned} \tag{4}$$

To further validate the improvement of the proposed circuit, the equivalent circuits of the 6T2C circuit and the proposed circuit shown in Fig. 12 are measured. Fig. 13(a) displays the configuration of the measurement platform. Two fabricated TFTs, which operate in the saturation region and linear region, respectively, are connected in series to represent T1 and T2 in the both circuits. Nodes A and V_{SS} of T1 and nodes D and E of T2 in the measurement are as the same as the voltages listed in Table II. Fig. 13(b) exhibits the measured results of the two equivalent circuits. When the current is 2.0070 mA and the voltage at node D is 9 V, the voltage at node C is 2.792 V.

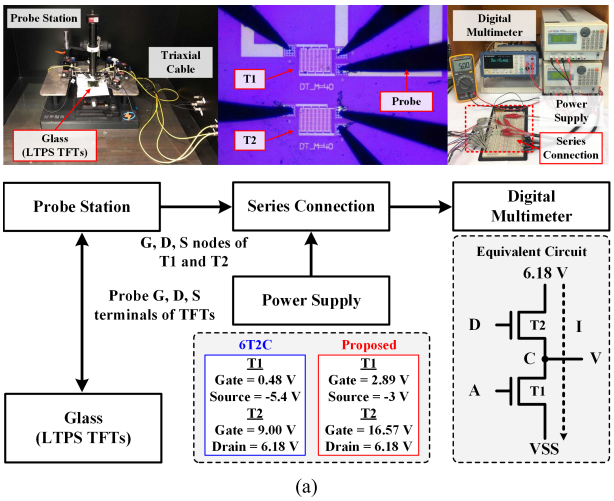

(a)

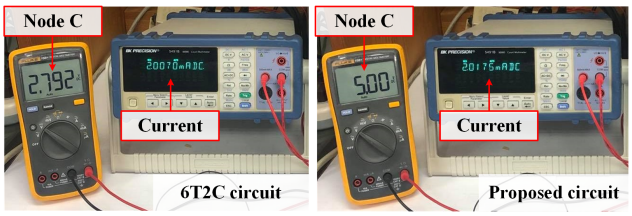

(b)

Fig. 13. (a) System of measurement platform. (b) Measured results of two equivalent circuits.

TABLE III
COMPARISON BETWEEN PROPOSED AND PREVIOUSLY DEVELOPED CIRCUITS

	[11]	[12]	[14]	This work
Driving method	AM	AM	AM	AM
TFT process	a-Si:H	LTPS	a-Si:H	LTPS
Number of LED per zone	4	1	1	1
Number of TFT on current path	1	1	1	2
V_{TH} compensation	No	No	No	Yes
V_{SS} compensation	No	No	No	Yes
Dimming zone	432	1024	5184	2304
Panel size (inch)	21.2	2.02	75	2.89

Thus, the V_{DS} of T2 is 3.388 V; when the current is 2.0175 mA and the voltage at node D is 16.57 V, the voltage at node C becomes 5.00 V, and thereby the V_{DS} of T2 is 1.18 V. It can be seen that the measured results highly meet the simulated results and verify the feasibility of the proposed circuit for reducing the power consumption of the AM mini-LED backlit module.

C. Comparison Between Proposed and Previously Developed Circuits

Table III compares the proposed circuit and the state-of-the-art circuits that are used in AM mini-LED backlight. In previous works [11], [12], [14], conventional 2T1C circuits have been used to drive mini-LEDs, generating a nonuniform driving currents in each BLU. Although [15], [16] implemented the compensation structure in the AM mini-LED display, the issues concerning the power consumption that are raised by the switching TFTs must still be improved. In contrast, by compensating for the V_{TH} variation and V_{SS} I–R rise, the proposed circuit provides a stable driving current for a mini-LED, providing more uniform brightness than the conventional 2T1C circuit. Also, without adjusting the voltage level of the scan signals or increasing the size of the TFTs, the proposed circuit reduces the V_{DS} of the switching TFT, improving the power consumption of the mini-LED backlight.

V. CONCLUSION

This work proposes a new AM mini-LED driving circuit for HDR LCDs. The proposed circuit can compensate for the V_{TH} variation in an LTPS TFT and the V_{SS} I–R rise to produce a highly uniform driving current that flows through the mini-LED. Furthermore, by reducing the V_{DS} of the switching TFT that is placed on the driving current path, the proposed circuit can generate the required I_{LED} despite reducing the total voltage across the circuit. Simulated results demonstrate that the proposed circuit can improve the brightness uniformity of the mini-LED backlight from 59% to 82% with V_{TH} and V_{SS} variations. The power consumption of each driving circuit is reduced by 16.67% relative to that achieved with a conventional AMOLED pixel structure. In comparison to a 6T2C circuit, the measurements verify that the total voltage across the proposed circuit is 2.4 V lower when the driving currents of both equivalent circuits are about 2 mA. These results demonstrate the feasibility of the proposed mini-LED driving circuit for use in an LCD BLU with uniform brightness and low power consumption.

REFERENCES

[1] H.-W. Chen, J.-H. Lee, B.-Y. Lin, S. Chen, and S.-T. Wu, "Liquid crystal display and organic light-emitting diode display: Present status and future perspectives," *Light, Sci. Appl.*, vol. 7, no. 3, Mar. 2018, Art. no. 17168, doi: 10.1038/lsa.2017.168.

[2] Y. Huang, E.-L. Hsiang, M.-Y. Deng, and S.-T. Wu, "Mini-LED, micro-LED and OLED displays: Present status and future perspectives," *Light: Sci. Appl.*, vol. 9, no. 1, pp. 1–6, Jun. 2020, doi: 10.1038/s41377-020-0341-9.

[3] J. Herrnsdorf *et al.*, "Active-matrix GaN micro light-emitting diode display with unprecedented brightness," *IEEE Trans. Electron Devices*, vol. 62, no. 6, pp. 1918–1925, Jun. 2015, doi: 10.1109/TED.2015.2416915.

[4] W. Guo *et al.*, "The impact of luminous properties of red, green, and blue mini-LEDs on the color gamut," *IEEE Trans. Electron Devices*, vol. 66, no. 5, pp. 2263–2268, May 2019, doi: 10.1109/TED.2019.2906321.

[5] M. Y. Soh *et al.*, "Design and characterization of micro-LED matrix display with heterogeneous integration of GaN and BCD technologies," *IEEE Trans. Electron Devices*, vol. 66, no. 10, pp. 4221–4227, Oct. 2019, doi: 10.1109/TED.2019.2933552.

[6] C.-H. Huang *et al.*, "Research on a novel GaN-based converted mini-LED backlight module via a spectrum-decouple system," *IEEE ACCESS*, vol. 8, pp. 138823–138833, 2020, doi: 10.1109/ACCESS.2020.3010026.

[7] G. Tan, Y. Huang, M.-C. Li, S.-L. Lee, and S.-T. Wu, "High dynamic range liquid crystal displays with a mini-LED backlight," *Opt. Exp.*, vol. 26, no. 13, pp. 16572–16584, Jun. 2018, doi: 10.1364/OE.26.016572.

[8] T. Masuda *et al.*, "28-3: Mini-LED backlight for HDR compatible mobile displays," in *SID Symp. Dig. Tech. Papers*, Jun. 2019, pp. 390–393, doi: 10.1002/sdtp.12939.

[9] E. Guan *et al.*, "17-3: A novel pixel-level local dimming backlight system for HDR display based on mini-LED," in *SID Symp. Dig. Tech. Papers*, Aug. 2020, pp. 231–234, doi: 10.1002/sdtp.13846.

[10] C.-L. Ting, C.-K. Wei, K.-Y. Kao, L.-W. Mau, H.-T. Chen, and M. Shibazaki, "Active matrix driving mini-LED device," in *IDW Tech. Dig.*, 2019, pp. 425–428, doi: 10.36463/idw.2019.0425.

[11] B. Liu *et al.*, "An active matrix mini-LEDs backlight based on a-Si TFT," in *IDW Tech. Dig.*, Jul. 2019, pp. 652–654.

[12] Y.-E. Wu, M.-H. Lee, Y.-C. Lin, C. Kuo, Y.-H. Lin, and W.-M. Huang, "Active matrix mini-LED backlights for 1000PPI VR LCD," in *SID Symp. Dig. Tech. Papers*, Jun. 2019, pp. 562–565, doi: 10.1002/sdtp.12982.

[13] J.-J. Su *et al.*, "An overview of solutions for achieving HDR LCDs," in *SID Symp. Dig. Tech. Papers*, 2020, pp. 224–227, doi: 10.1002/sdtp.13844.

[14] H. Xu *et al.*, "AM MLED backlight units on glass for 75-inch LCD displays," in *SID Symp. Dig. Tech. Papers*, 2020, pp. 122–125, doi: 10.1002/sdtp.13820.

[15] W.-S. Shin *et al.*, "A driving method of pixel circuit using a-IGZO TFT for suppression of threshold voltage shift in AMLED displays," *IEEE Electron Device Lett.*, vol. 38, no. 6, pp. 760–762, Jun. 2017, doi: 10.1109/LED.2017.2699669.

[16] B. Liu, Q. Liu, J. Liu, F. Zhu, and H. Zhou, "A new compensation pixel circuit based on a-Si TFTs," in *Proc. IEEE Int. Conf. Electron. Technol.*, May 2020, pp. 123–126, doi: 10.1109/ICET49382.2020.9119591.

[17] C.-L. Lin, C.-C. Hung, P.-S. Chen, P.-C. Lai, and M.-H. Cheng, "New voltage-programmed AMOLED pixel circuit to compensate for nonuniform electrical characteristics of LTPS TFTs and voltage drop in power line," *IEEE Trans. Electron Devices*, vol. 61, no. 7, pp. 2454–2458, Jul. 2014, doi: 10.1109/TED.2014.2325612.

[18] Y.-H. Tai, C.-H. Lin, S. Yeh, C.-C. Tu, and K. S. Karim, "LTPS active pixel circuit with threshold voltage compensation for X-ray imaging applications," *IEEE Trans. Electron Devices*, vol. 66, no. 10, pp. 4216–4220, Oct. 2019, doi: 10.1109/TED.2019.2933225.

[19] M. Bagheri, S. J. Ashitani, and A. Nathan, "Fast voltage-programmed pixel architecture for AMOLED displays," *J. Display Technol.*, vol. 6, no. 5, pp. 191–195, May 2010, doi: 10.1109/JDT.2010.2044015.

[20] C.-L. Lin, C.-C. Hung, W.-Y. Chang, M.-H. Cheng, P.-Y. Kuo, and Y.-C. Chen, "Voltage driving scheme using three TFTs and one capacitor for active-matrix organic light-emitting diode pixel circuits," *J. Display Technol.*, vol. 8, no. 10, pp. 602–608, Oct. 2012, doi: 10.1109/jdt.2012.2209110.

[21] C.-L. Lin, C.-C. Hung, P.-Y. Kuo, and M.-H. Cheng, "New LTPS pixel circuit with AC driving method to reduce OLED degradation for 3D AMOLED displays," *J. Display Technol.*, vol. 8, no. 12, pp. 681–683, Dec. 2012, doi: 10.1109/JDT.2012.2225017.

[22] W.-J. Wu *et al.*, "High-speed voltage-programmed pixel circuit for AMOLED displays employing threshold voltage one-time detection method," *IEEE Electron Device Lett.*, vol. 34, no. 9, pp. 1148–1150, Sep. 2013, doi: 10.1109/LED.2013.2271908.

[23] J.-P. Lee, H.-S. Jeon, D.-S. Moon, and B. S. Bae, "Threshold voltage and IR drop compensation of an AMOLED pixel circuit without a V_{DD} line," *IEEE Electron Device Lett.*, vol. 35, no. 1, pp. 72–74, Jan. 2014, doi: 10.1109/LED.2013.2289315.

[24] C.-L. Lin, Y.-T. Liu, C.-E. Lee, P.-S. Chen, T.-C. Chu, and C.-C. Hung, "A-InGaZnO active-matrix organic LED pixel periodically detecting thin-film transistor threshold voltage once for multiple frames," *IEEE Electron Device Lett.*, vol. 36, no. 11, pp. 1166–1168, Nov. 2015, doi: 10.1109/LED.2015.2480861.

[25] N.-H. Keum, S.-K. Hong, and O.-K. Kwon, "An AMOLED pixel circuit with a compensating scheme for variations in subthreshold slope and threshold voltage of driving TFTs," *IEEE J. Solid-State Circuits*, vol. 55, no. 11, pp. 3087–3096, Nov. 2020, doi: 10.1109/JSSC.2020.3014149.

[26] F. Gou, H. Chen, M.-C. Li, S.-L. Lee, and S.-T. Wu, "Motion-blur-free LCD for high-resolution virtual reality displays," *J. Soc. Inf. Display*, vol. 26, no. 4, pp. 223–228, Apr. 2018, doi: 10.1002/jsid.662.